Published online 13 April 2021

Nucleic Acids Research, 2021, Vol. 49, No. 8 ***4599–4612***
doi: 10.1093/nar/gkab243

DNA polymerase D temporarily connects primase to the CMG-like helicase before interacting with proliferating cell nuclear antigen

Keisuke Oki[1], Takeshi Yamagami[1], Mariko Nagata[1], Kouta Mayanagi[2], Tsuyoshi Shirai[3], Naruhiko Adachi[4], Tomoyuki Numata[1], Sonoko Ishino[1,*] and Yoshizumi Ishino[1,*]

[1]Department of Bioscience and Biotechnology, Graduate School of Bioresource and Bioenvironmental Sciences, Kyushu University, Fukuoka, Japan, [2]Medical Institute of Bioregulation, Kyushu University, 3-1-1 Maidashi, Higashi-ku, Fukuoka-shi, Fukuoka 812-8582, Japan, [3]Department of Bioscience, Nagahama Institute of Bio-Science and Technology, Tamura 1266, Nagahama, Shiga 526-0829, Japan and [4]Structure Biology Research Center, Institute of Materials Structural Science, High Energy Accelerator Research Organization, 1-1 Oho, Tsukuba, Ibaraki 305-0801, Japan

Received February 05, 2021; Revised March 23, 2021; Editorial Decision March 23, 2021; Accepted March 25, 2021

ABSTRACT

The eukaryotic replisome is comprised of three family-B DNA polymerases (Polα, δ and ε). Polα forms a stable complex with primase to synthesize short RNA-DNA primers, which are subsequently elongated by Polδ and Polε in concert with proliferating cell nuclear antigen (PCNA). In some species of archaea, family-D DNA polymerase (PolD) is the only DNA polymerase essential for cell viability, raising the question of how it alone conducts the bulk of DNA synthesis. We used a hyperthermophilic archaeon, *Thermococcus kodakarensis*, to demonstrate that PolD connects primase to the archaeal replisome before interacting with PCNA. Whereas PolD stably connects primase to GINS, a component of CMG helicase, cryo-EM analysis indicated a highly flexible PolD–primase complex. A conserved hydrophobic motif at the C-terminus of the DP2 subunit of PolD, a PIP (PCNA-Interacting Peptide) motif, was critical for the interaction with primase. The dissociation of primase was induced by DNA-dependent binding of PCNA to PolD. Point mutations in the alternative PIP-motif of DP2 abrogated the molecular switching that converts the archaeal replicase from *de novo* to processive synthesis mode.

INTRODUCTION

Replicative polymerases coordinate to ensure rapid and accurate DNA replication. One of the most fundamental features of a DNA replicase is that it can only add deoxyribonucleotides (dNTP) to the 3′-end of an already existing daughter strand. The absence of a *de novo* synthesis function necessitates a specialized DNA-dependent RNA polymerase, known as primase. Two types of primase provide short RNA primer synthesis and transfer to the DNA polymerase extension reaction (1). Bacterial DnaG primase is a single protein often complexed with the replicative helicase. Eukaryotic/archaeal primases are heterodimers of a small subunit (p48 or PriS), containing the catalytic centre and a large subunit (p58 or PriL) that regulates primase activity.

The p48-like protein (p41) found in *Pyrococcus furiosus* did not synthesize short RNA but preferentially utilized deoxynucleotides to synthesize DNA strands up to several kilobases in length, by itself, *in vitro* (2). A neighbouring gene encoded a protein with very weak similarity to the eukaryotic p58 protein. The gene product designated p46 forms a stable complex with p41 and synthesize a short RNA primer *in vitro* (3). Subsequently, short RNA primer was identified within *Pyrococcus* cells, suggesting that short RNA is universally synthesized and utilized for DNA replication in the three domains of life (4). Further studies characterized p41 and p46 homologs in other archaea as introduced in the recent review articles (1,5,6). The small and large subunits are now generally called as PriS and PriL, respectively.

In the eukaryotic replisome, the primase and family-B DNA polymerases, Polα, δ and ε, mediate nascent-strand synthesis (7). The initial step relies on the Polα-primase complex, comprised of the p180 catalytic subunit (Pol1), the second p70 subunit (Pol12) of Polα and the p58 and p48 subunits of primase (8). Polα-primase interacts with CMG (Cdc45–MCM2–7–GINS) helicase via Ctf4 to form the replisome (9). As helicase unwinds the template DNA,

*To whom correspondence should be addressed. Tel: +81 92 802 4715; Fax: +81 92 802 4696; Email: ishino@agr.kyushu-u.ac.jp
Correspondence may also be addressed to Sonoko Ishino. Tel: +81 92 802 4714; Fax: +81 92 802 4696; Email: sonoko@agr.kyushu-u.ac.jp

the p48–p58 primase mediates *de novo* synthesis of 7–12 ribonucleotide oligomers that are handed off to Polα, which extends the oligomer to 30 deoxyribonucleotides (10). The Polα-primase interaction is mediated by the C-terminal portion of p180 and the N-terminal portion of p58 and is essential for efficient transfer of the RNA primer to DNA strand extension (11). In *Saccharomyces cerevisiae,* truncation of 16 amino acids from the C-terminus of p180 ortholog Pol12 prevents Polα-primase complex formation, thereby blocking proliferation (12). Subsequently, the RNA-DNA primers are extended on both templates by Polε and Polδ (13,14), supported by proliferating cell nuclear antigen (PCNA). PCNA is the sliding clamp that encircles double-stranded DNA (dsDNA) in its central channel and tethers DNA polymerases to the DNA (15). Polε directly binds GINS (16,17) and Polδ interacts with Polα (18), contributing to the efficient transfer of nascent strands. Recent genetic analyses showed that Polδ also mediates leading-strand synthesis at replication origins, and the nascent strands can be handed off from primase → Polα → Polδ → Polε (19,20). Since the Okazaki fragment in Archaea and Eukarya is ∼100–200 bp, frequently repeated synthesis of the primer and transfer of its 3′-end to processive DNA polymerases must be efficient.

All three eukaryotic replicases share a common structural feature. In addition to the family-B structure including zinc finger motifs in the C-terminus of the catalytic subunits, their second subunits, p70 of Polα, p50 of Polδ, and p59 of Polε, are also conserved and belong to the calcineurin-like phosphodiesterase superfamily (21–23). Bioinformatics and structural analyses have revealed that these features are strikingly similar to the C-terminal domain of DP2 (catalytic subunit) and DP1 (second subunit) of the archaeal family-D DNA polymerase (PolD) (24,25). PolD was initially discovered from *P. furiosus* as a unique DNA polymerase (26), and is now recognized as being widely conserved among Archaea except in the phylum Crenarchaeota (27). Genetic studies of *T. kodakarensis* and *M. maripaludis* revealed that PolD is the only DNA polymerase essential for cell viability (28,29), and thus seems to be the *bona fide* replicative DNA polymerase. In fact, PolD directly binds CMG-like helicase in the archaeal replisome. The homohexameric MCM helicase is stimulated by GINS and GAN (Gins Associated Nuclease, the archaeal ortholog of Cdc45/RecJ) (30–34). Several studies have reported the interaction of GINS and PolD (35–37).

Previous *in vitro* studies demonstrated that PolD directly extends RNA primers, as Polα does (38,39), and processively extends DNA strands with PCNA, as Polδ and Polε do (38,40,41). However, the molecular mechanism of coordinating the sequence of primer synthesis, hand-off and elongation in Archaea has been unclear. A study on *P. abyssi* identified two PIP (PCNA-Interacting Peptide) motifs, cPIP (canonical PIP) and iPIP (internal PIP), in the C-terminal region of DP2. Although cPIP interacted with primase and PCNA, cryo-EM showed that iPIP interacts with PCNA during processive DNA synthesis. The authors proposed that cPIP is the master switch between the initiation and processive phases of the replisome in *P. abyssi,* and discussed the similarity of the archaeal interaction with those of eukaryotic Polα and primase (42).

Here, we demonstrate that *T. kodakarensis* PolD temporarily connects primase to the CMG-like helicase before processive synthesis with PCNA. Purified PolD and primase made a stable four-subunit complex (DP1, DP2, PriS and PriL), and cryo-EM revealed their flexible association. Primase-bound PolD simultaneously interacted with GINS, *in vivo* and *in vitro*, suggesting the formation of an archaeal replisome containing helicase, polymerase and primase. We also found that the interactions of DP1–PriS and DP2–PriL mediate stable PolD–primase complex formation. A conserved hydrophobic motif (corresponding to cPIP) at the extreme C-terminus of DP2 was essential to the primase interaction. Moreover, PolD could not simultaneously bind primase and PCNA; primase dissociation was induced by DNA-dependent binding of PCNA to PolD. Point mutations in iPIP abolished molecular switching. These findings support the hypothesis that partner exchange on DP2 switches the function of PolD from *de novo* synthesis to processive elongation.

MATERIALS AND METHODS

Recombinant protein preparations

The preparation of recombinant PolD, PolDΔC11 (DP2Δ1314–1324), PCNA1 (TK0535) and GINS was described previously (43). Primase (PriS–PriL complex) was prepared by cloning the genes encoding PriS and PriL from *T. kodakarensis* into pETDuet-1 (Novagen). *Escherichia coli* BL21-CodonPlus (DE3)-RIL (Agilent Technologies) harbouring the plasmid were cultured in Luria-Bertani medium containing 50 μg/ml ampicillin and 34 μg/ml chloramphenicol at 37°C to an OD_{600} of 0.3. Gene expression was induced by adding IPTG to a final concentration of 1 mM and incubating at 25°C for 18 h. The cells were collected, resuspended in buffer A (50 mM Tris–HCl, pH 8.0, 2 mM DTT) including 0.3 M NaCl and disrupted by sonication. The complex was purified by heat treatment at 80°C for 20 min. The heat-resistant fraction was treated with 0.15% (v/v) polyethyleneimine in buffer A containing 1 M NaCl to remove nucleic acids. The soluble fraction was precipitated with 80% saturated $(NH_4)_2SO_4$ and resuspended in buffer A containing 1.65 M $(NH_4)_2SO_4$. The soluble fraction was applied to a HiTrap Butyl HP column (GE Healthcare) and eluted with a linear gradient of 1.65–0 M $(NH_4)_2SO_4$ in buffer A. The fractions containing complex were dialysed against buffer A and applied to a HiTrap Heparin HP column (GE Healthcare). The column was developed with a linear gradient of 0–1 M NaCl in buffer A. The fractions containing complex were dialysed against buffer A again and then applied to a BioPro IEX SmartSep Q10 column (YMC). The column was developed with a linear gradient of 0–1 M NaCl in buffer A, and the fractions containing pure stoichiometric primase were pooled and frozen in liquid nitrogen until use. Each subunit of the primase was prepared individually. The genes encoding PriS and PriL were cloned into pET-21a(+) and pET-24a(+) (Novagen), respectively. Gene expression, protein overproduction and purification were conducted as described for the primase complex with some modifications. Briefly, for PriS, the HiTrap butyl HP column was developed with a linear gradient of 1.65–0 M

$(NH_4)_2SO_4$ in buffer A, followed by elution with deionised water. The fractions containing PriS were dialysed against buffer A and applied to an HiTrap Heparin HP column. The column was developed with a linear gradient of 0–1 M NaCl in buffer A, and the fractions containing pure PriS were pooled. For PriL, the HiTrap butyl HP column was developed with a linear gradient of 1.65–0 M $(NH_4)_2SO_4$ in buffer A. The fractions containing PriL were dialysed against buffer A and applied to the HiTrap Q HP column (GE Healthcare). The column was developed with a linear gradient of 0–1 M NaCl in buffer A, and the fractions containing pure PriL were pooled.

Site-specific mutagenesis

PCR-mediated mutagenesis was performed with a QuikChange™ site-directed mutagenesis kit (Agilent Technologies) to prepare PolD variants containing mutations at two PIP motifs (Q1206A/L1209A/M1210A and L1318A/F1321A/F1322A). The template DNA was pET21a-DP2 (41). The mutations were confirmed by nucleotide sequencing. The mutagenesis primers (TK1903-iPIP-F/TK1903-iPIP-R and TK1903-cPIP-F/TK1903-cPIP-R) are listed in Supplementary Table S1. Expression and purification of mutant PolDs were performed as described above.

Native PAGE

Native PAGE was used to detect interactions of PolD with primase and GINS. Each protein, alone and in combination, was incubated at 60°C for 2 min. The protein solutions were mixed with 5× gel-loading buffer (15% Ficoll, 0.1% bromophenol blue), separated by native-5% PAGE in TBE and stained with coomassie brilliant blue (CBB).

Yeast two-hybrid assay

A yeast two-hybrid (Y2H) detection system (Matchmaker™ Gold Yeast Two-hybrid System, Matchmaker GAL4 Two-Hybrid System 3, Clontech) was used to detect interactions of PolD (DP1, DP2) with primase (PriS, PriL) and various DP2 fragments with PriL. The plasmid pGBKT7, encoding the GAL4 DNA binding region, and the plasmid pGADT7, encoding the activation domains, were used to prepare plasmids containing the *T. kodakarensis* gene encoding DP1, DP2, PriS and PriL. Co-transformations of the Y2H Gold cells with pGBKT7 and pGADT7 were performed according to the manufacturer's protocol (Clontech Matchmaker manual). Cell suspensions (3 μl of 2×10^6 cells/ml) of each strain were spotted onto synthetic defined (SD) plates without Leu and Trp for non-selection and without Leu, Trp and His for selection. The agar plates were incubated at 30°C for 4 days. Growing cells indicated interactions between the two proteins produced by the plasmids used for co-transformation.

Surface plasmon resonance (SPR) analysis

The Biacore J system (GE Healthcare) was used to test the physical interactions of PolD with primase, PriS or PriL. PolD was fixed on a CM5 Sensor Chip (GE Healthcare) according to manufacturer's instructions. Immobilized PolD showed 6662 RU. To measure the kinetic parameters, purified primase, PriS or PriL in running buffer (50 mM Tris–HCl, pH8.0, 0.3 M NaCl, 0.1% IGEPAL), was passed across the PolD-immobilized chip for 120 s at a continuous flow rate of 30 μl/min at 25°C. The bound analytes were removed by washing with regeneration buffer (50 mM Tris–HCl, pH8.0, 1 M NaCl, 0.1% IGEPAL) at the end of each cycle. Equilibrium constants (K_D) were determined from the association and dissociation curves of the sensorgrams using BIAevaluation software (ver. 4.1, GE Healthcare).

Gel-filtration chromatography

Gel-filtration chromatography was performed using the SMART system (Amersham Pharmacia). Each purified recombinant protein and mixtures (each 2.4 μM) were incubated for 3 min at 60°C. Aliquots (20 μl) of each protein solution was applied to a Superose 6 PC 3.2/30 column (GE Healthcare) and eluted with buffer (50 mM Tris–HCl, pH 8.0 and 0.15 M NaCl). An aliquot (0.1 μl) of the protein solution and each eluted fraction (4 μl) were separated by 10% SDS-PAGE containing WIDE RANGE Gel Preparation Buffer (Nacalai Tesque), followed by silver staining. As an exception, in the experiments shown in Supplementary Figures S3 and S6, proteins (each 4.5 μM) were mixed in the presence or absence of equimolar primed-DNA (annealed deoxyoligonucleotides d29 and d45, Supplementary Table S1). Each solution (25 μl) was applied to the column. An aliquot (5 μl) of the applied solution and each eluted fraction were separated by 10% SDS-PAGE, followed by CBB staining. Standard marker proteins thyroglobulin (670 000), γ-globulin (158 000), ovalbumin (44 000) and myoglobin (17 000) were run as controls.

Nucleotide incorporation assay

A nucleotide incorporation assay was performed as described (26). The reaction was carried out in a 50 μl volume containing 20 mM Tris–HCl, pH8.0, 5 mM $MgCl_2$, 14 mM 2-mercaptoethanol, 0.2 mg/ml activated salmon sperm DNA, 0.2 mM dNTPs, 130 nM [methyl-^{3}H] dTTP (PerkinElmer) and protein (10 nM PolD, 50 nM primase, 50 nM GINS) to initiate the reaction. After incubation at 72°C for 2, 4, 6 and 8 min, aliquots (10 μl) of the reaction solution were spotted onto DE81 filters (GE Healthcare). The filters were washed three times with 5% Na_2HPO_4 and dried. Incorporated radioactivity was measured with a scintillation counter (AccuFLEX LSC-8000, Hitachi). Incorporated dNTPs in the spotted solutions were quantified (Figure 3).

Immunoprecipitation assay

T. kodakarensis was cultured in artificial seawater (ASW) supplemented with 5 g/l yeast extract and tryptone and 5 g/l sodium pyruvate (Pyr) at 85°C and harvested at the early exponential phase by centrifugation for 10 min at 5000 × *g*. The cells (4×10^{10}) were resuspended in 2 ml lysis buffer (50 mM Tris–HCl buffer, pH 7.0, 0.5 mM DTT, 10% glycerol, 0.1 mM EDTA, 50 mM NaCl and 0.1% Tween 20)

to a final concentration of 2×10^{10} cells/ml and disrupted by sonication. Extracts were obtained by centrifugation for 10 min at 23 000 × *g*. Polyclonal anti-PolD, anti-primase and anti-Gins23 antisera were raised independently by immunizing rabbits with the purified recombinant proteins as antigens. A portion (20 μl) of Protein A Sepharose FF (GE Healthcare) was washed three times with phosphate-buffered saline–Tween 20 (PBS-T: 10 mM sodium phosphate, pH 7.5, 150 mM NaCl and 0.1% Tween 20), mixed with 500 μl PBS-T containing 100 μl of each antiserum and incubated on a rotating wheel at room temperature for 1 h. Each mixture was washed three times with 500 μl 0.2 M triethanolamine, pH 8.0. Each antibody was cross-linked to rProtein A Sepharose with 10 mM dimethyl sulfide (Thermo Fisher Scientific). After equilibration of the antibody-conjugated rProtein A Sepharose with lysis buffer, an aliquot of the cell extract (8×10^9 cells) was added. The mixture was incubated on a rotating wheel at room temperature for 1 h. The precipitates were washed three times with lysis buffer, and the immunoprecipitated proteins were eluted with 40 μl gel-loading solution containing 50 mM Tris–HCl, pH 6.8, 10% glycerol, 5% β-mercaptoethanol, 0.2% bromophenol blue and 2% SDS. The eluted proteins were separated by SDS-PAGE, followed by western blot analysis. The proteins on the gel were transferred onto a polyvinylidene difluoride (PVDF) membrane (Bio-Rad) using a Trans-Blot Turbo Transfer System (Bio-Rad) and reacted with the anti-PolD, anti-primase, anti-Gins51 and anti-Gins23 antisera. Anti-Rabbit IgG HRP (Rabbit True-Blot, Rockland Immunochemicals) was used as the secondary antibody. The proteins were visualized by an enhanced chemiluminescence system (Millipore), and images were obtained and quantified with a LAS-3000 image analyser (Fujifilm).

Electron microscopy and single-particle image analysis

The purified PolD and PriS–PriL proteins were mixed in a solution containing 50 mM Tris–HCl (pH 8.0), 150 mM NaCl, at 25°C for 20 min and loaded onto a gel-filtration column. Superdex 200 5/150 (GE Healthcare) was used instead of Superose 6 PC 3.2/30 for this experiment. The complex solution (3 μl), eluted at the peak fraction was applied to a holey carbon (Quantifoil R1.2/1.3 Au 200) grid for rapid freezing. Grids were glow discharged for 1 min by an HDT-400 hydrophilic treatment device (JEOL, Tokyo, Japan) before usage. Rapid freezing was performed using Vitrobot (FEI) freezing robots. Frozen-hydrated samples were first examined by Polara electron microscopy (FEI) at 200 kV accelerating voltage to optimize the sample preparation conditions. Images were captured using an UltraScan 4k CCD camera (GATAN). Image datasets of the PolD–primase complex were collected on a Talos Arctica electron microscope (Thermo Fisher Scientific) under 200 kV accelerating voltage. EPU software (Thermo Fisher Scientific) was used for fully automated data collection. Images were recorded by Falcon 3EC direct electron detector (Thermo Fisher Scientific) in electron counting mode at a nominal magnification of 120 000×, corresponding to 0.88 Å/pixel on the specimen with 52.79 s total exposure time. The nominal defocus range was −1.0 to −2.5 μm. Intermediate frame fractions were recorded every 1.35 s, giving an accumulated dose of 49.92 electrons/Å^2 and a total of 39 fractions per image (i.e. 1.28 electrons/Å^2 dose per fraction). Movie frames of the PolD–primase complex were aligned to correct the dose-induced and dose-weighted motions of the specimens using MotionCor2 (44). The Contrast Transfer Function was determined for each image using the Gctf program (45). CrYOLO (46) was used to pick particles from the images automatically, and the output coordinates were used for the Relion particle extraction programme (47). A total of 363,812 particles were extracted from 2,373 PoD–primase complex images. Three rounds of 2D classification were performed to remove particles classified as 'bad' from the data set. In total, 311 578 particles were subjected to the Relion 3D classification (Class3D) and refinement procedure. The initial reference 3D map of the complex for the first round was reconstructed by the Relion 3D init procedure, and 85,888 particle images were used to reconstruct the final map. The final map was sharpened by applying a negative B-factor (−500) and corrected for the MTF of the Falcon 3EC detector. The resolution of the final maps was estimated by gold standard FSC using FSC = 0.143 criteria.

3D structure model construction of PolD-primase-DNA

The 3D model of the PolD–primase–DNA/RNA complex was constructed by assembling several known structures and applying the homology modelling method. The structure of the *T. kodakarensis* PolD–PCNA–dsDNA complex (PDB ID: 6KNB) (43) was first fit into the density map. The primase (PriS–PriL) complex was modelled by using MODELLER (48) based on the heterodimeric structure of the *S. solfataricus* core primase (PDB ID: 1ZT2) (49). The primase–DNA/RNA(primer)–UTP(substrate) model was constructed by referring to the *P. horikoshii* DNA primase–UTP complex (PDB ID: 1V34) and C-terminal domain of the human DNA primase large subunit complexed with DNA template/RNA primer (PDB ID: 5F0Q) (50,51). The primase–DNA/RNA–UTP complex model was then docked to the PolD–PCNA–dsDNA complex by fitting the PriS subunit of the primase into the remaining density. The actual cPIP position is not visible in the cryo-EM structures of the PolD–PCNA–dsDNA complex (43). We have experimentally shown that primase binds to cPIP of DP2 in this study. PCNA and primase can exchange by converting the position of the flexible C-terminal region of DP2. Therefore, the cPIP position relative to primase was predicted by remodelling iPIP into cPIP in the form A density of the PolD–PCNA–dsDNA complex.

RESULTS

Primase does not bind GINS directly in *T. kodakarensis*

The first question in understanding archaeal replisome structure and function was how archaeal primase is integrated into the replisome. In *E. coli,* the replicative helicase DnaB directly interacts with DnaG primase (52,53). Similarly, the crenarchaeon *Sulfolobus solfataricus* primase interacts with GINS, a CMG helicase component, as demonstrated by Y2H and pull-down experiments (54). We used

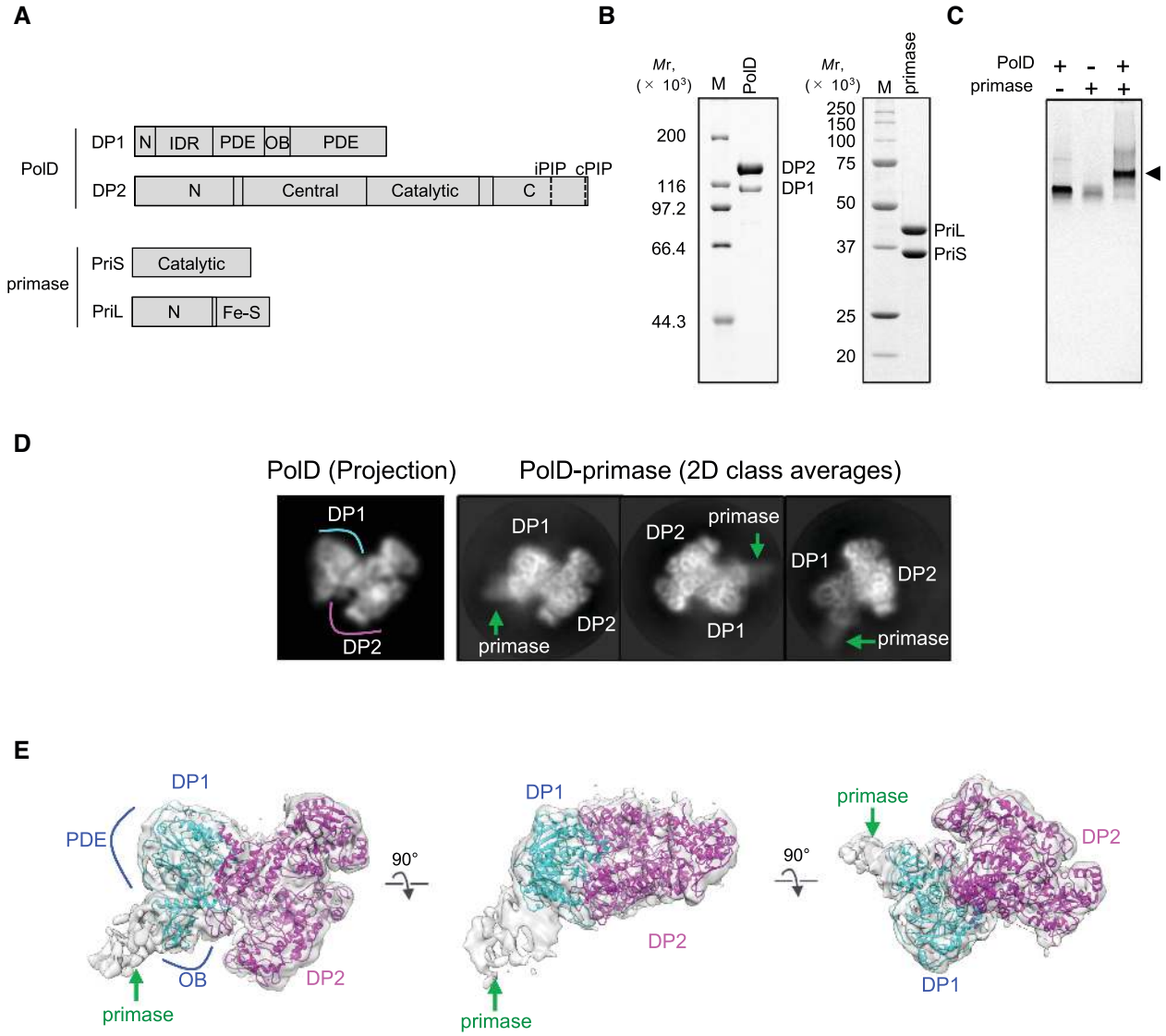

Figure 1. Complex formation of DNA polymerase (PolD) and primase. (**A**) Subunit compositions and domain organisations of PolD and primase from *T. kodakarensis*. N: N-terminal, IDR: intrinsically disordered region, PDE: phosphodiesterase, OB: oligonucleotide/oligosaccharide binding, C: C-terminal, iPIP: internal PIP, cPIP: canonical PIP, Fe–S: iron–sulfur cluster. (**B**) Purification of the recombinant PolD and primase proteins. Purified PolD (2.8 μg) and primase (2 μg) were subjected to SDS-7.5% PAGE and 10% PAGE, respectively, followed by Coomassie Brilliant Blue (CBB) staining. Protein size markers were run in lane M, and their sizes are indicated on the left side of the gel. (**C**) Complex formation of PolD and primase was analysed by native PAGE. Each protein (12 pmol) and their mixture were analysed. The black arrowhead indicates the shifted band, suggesting the formation of PolD–primase complex. (**D**) Comparison between a projection image of PolD (PDB: 6KNB), and representative 2D class averages of the PolD–primase complex revealed by cryo-EM analysis. Extra density corresponding to primase is highlighted with a green arrow. (**E**) 3D structure of the PolD–primase complex. We applied the PolD part of PDB:6KNB as a rigid model to construct a docking model. The atomic models of DP1 and DP2 are cyan and magenta, respectively.

native PAGE and gel-filtration chromatography and discovered that *T. kodakarensis* primase does not form a stable complex with the replicative helicase (Supplementary Figure S1). *T. kodakarensis,* an euryarchaeon, may have different mechanism to form a functional replisome.

Direct interaction between PolD and primase

Previous *in vitro* analyses revealed that PolD uses RNA primer to extend the strand using deoxyribonucleotides (38,39). A comprehensive analysis of protein-protein interactions in the cell extracts of *P. abyssi* showed that PriL co-isolated with the His-tagged DP2 subunit of PolD (36). To determine directly whether PolD physically interacts with primase, we used purified PolD and primase (Figure 1A, B) to perform a native PAGE gel-shift assay. As shown in Figure 1C, the protein bands for PolD and primase shifted from their original positions when the two proteins were mixed, suggesting the formation of a PolD–primase complex. We visualized the PolD–primase complex by gel filtration (as described below) and cryo-EM. Representative 2D class averages are shown in Figure 1D. The image was similar to that of PolD alone (55), or a projection image of PolD extracted from PolD–PCNA–DNA complex (43, PDB:6KNB). However, an extra density was found extending from the region, corresponding to the DP1 subunit. Fig-

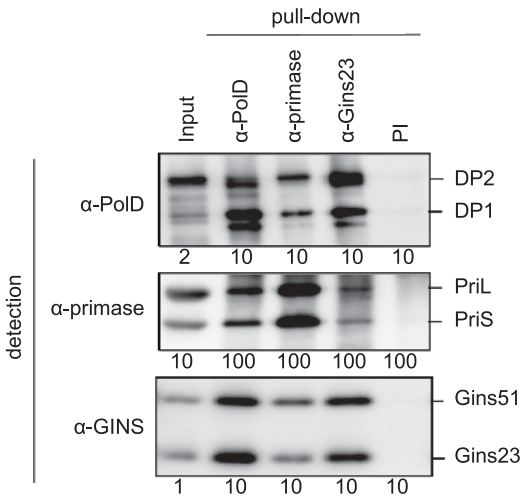

Figure 2. DNA polymerase (PolD), primase and GINS make a complex in *T. kodakarensis* cells. Immunoprecipitation of PolD, primase and GINS in *T. kodakarensis* cell extract. The immunocomplexes were captured individually with each antiserum from the whole-cell extract (as shown at the top) and separated by SDS–7.5% PAGE (PolD), SDS–10% PAGE (primase) or SDS–12.5% PAGE (GINS), followed by western blot analyses using these antisera (shown on the left side). The whole-cell extracts without immunoprecipitation (Input) and those precipitated after treatment with preimmune serum (PI) were also loaded as positive and negative controls, respectively. The ratio of the loading amounts is indicated at the bottom of the panels.

ure 1E shows the 7.1 Å resolution 3D map of PolD–primase complex. The atomic model of PolD was nicely fitted into the map. As suggested by the 2D class average, a protrusion extended from the OB (oligonucleotide/oligosaccharide-binding) domain of DP1 was suggested as the density from primase. These data support the hypothesis that PolD and primase directly bind and work as a primosome complex. The intensity of the primase region decreased with increasing distance from the interface with PolD, suggesting the primase moves remarkably easily within the complex.

PolD connects primase to helicase

The interaction between PolD and GINS has been suggested by comprehensive protein interaction analyses reported in *T. kodakarensis* (35) and *P. abyssi* (36) and also reported using purified proteins from *Thermococcus* sp. 4557 (37). We expected PolD to mediate the interaction between primase and helicase in the replisome. To investigate whether PolD, primase and GINS form a complex in *T. kodakarensis*, we first performed an immunoprecipitation experiment. Exponentially growing cells (OD_{660} = 0.3) were harvested, and the immunocomplexes were captured with anti-PolD, anti-primase or anti-Gins23 antibodies from the whole-cell extracts. All three proteins (PolD, primase and GINS) were co-precipitated with any of the three antibodies, suggesting that they are co-localized in the same complex (Figure 2).

Complex formation was also confirmed directly using purified recombinant proteins *in vitro*. The mixture of PolD, primase and GINS yielded a band shift relative to a single or two-protein mix on native PAGE (Figure 3A). Gel-filtration chromatography was performed to isolate the complex, and the elution profile indicated the formation of a ternary GINS–PolD–primase complex. A broad peak of the elution profile may suggest that several complexes with different stoichiometry of the component proteins were formed. However, the elution position of the main peak corresponded to a molecular weight >670 000 (Figure 3B). It is not easy to determine the stoichiometry of each component in the complex from the gel filtration. Our knowledge that GINS contains two Gins51 subunits (57), each of which binds DP1 subunit of PolD (37), may predict the formation of the $GINS_1$–$PolD_2$–$primase_2$ complex. The elution position of the main peak described above at least corresponds to the estimated molecular size of $GINS_1$–$PolD_2$–$primase_2$. Further analysis is needed to precisely determine the stoichiometry of each component in the complex.

To determine whether the GINS–PolD–primase complex retains enzymatic activity, we measured the nucleotide incorporation activity of PolD in the presence of primase and GINS (Figure 3C). The results showed that PolD retained full polymerase activity in either the presence or absence of primase and GINS. The possibility that only subcomplex displays activity should be considered carefully. However, the concentrations of proteins used for the assay should be sufficient to form a complex according to the calculated affinity (K_D values), as described below, and PolD probably retains full polymerase activity while forming a tight complex with primase and GINS. These results support that PolD connects primases to helicases by interaction with GINS, the component of the CMG-like helicase (33), in the archaeal replisome. Further studies are required to identify the real replisome in archaeal cells.

PolD–primase interaction

Y2H assays with subunits of each protein were used to investigate how PolD and primase interact. Colony formation was observed with DP1–PriS and DP2–PriL in the selection medium (Figure 4A). In this experiment, the DP1–DP2 interaction for PolD was clearly observed; however, PriS–PriL interaction for primase was not detected. This result was reproducible, and we have concluded that the bait and prey proteins constructed for this Y2H experiment were not suitable for the interaction of PriS and PriL. SPR analysis was used to confirm and quantify the binding affinity of these interactions. The sensorgram of primase and immobilized PolD showed stable binding with an apparent K_D of 43 nM (Figure 4B). SPR analysis under the same conditions using individual PriS and PriL proteins as analytes was performed to investigate the site of interaction and binding affinity (Figure 4B). Both subunits of the primase bound to PolD, but the apparent K_D value was 9-fold lower for PriL (0.16 μM) than PriS (1.4 μM), suggesting that stable complex formation relies more on the interactions of DP2–PriL than DP1–PriS.

PolD binds primase via the conserved hydrophobic motif at the C-terminus of DP2

We further performed additional Y2H experiments to map the site of DP2–PriL interaction. The DP2 protein was

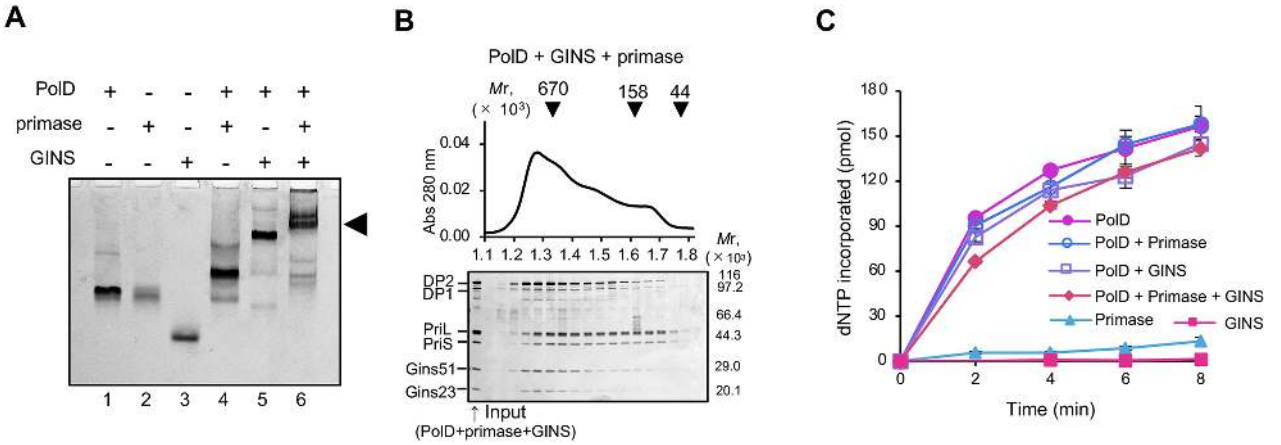

Figure 3. DNA polymerase (PolD), primase and GINS make a ternary complex, and it retained full nucleotide incorporation activity. (**A**) Complex formation of PolD, primase and GINS was analysed by native PAGE. Each purified protein (12 pmol) and mixtures of them were analysed. The black arrowhead indicates the shifted band, suggesting the formation of PolD–primase–GINS complex. (**B**) Complex formation of PolD, primase and GINS was analysed by a gel-filtration chromatography. The elution profiles, monitored by the absorbance at 280 nm, are shown. The peak positions of the marker proteins are indicated on the top. Aliquots of each fraction were subjected to SDS-PAGE followed by silver staining. (**C**) The nucleotide incorporation activity of PolD in the presence or absence of primase and GINS were analysed. The amount of incorporated deoxyribonucleotides (dNTP) was calculated and shown. Three independent experiments were carried out, and the SEM values are shown as vertical lines on the plots in each graph.

fragmented based on the structure and each fragment was used for bait to analyse the interaction. As shown in Figure 5A, only the C-terminal domain of DP2 (1000–1324) interacted with PriL. Recent cryo-EM analyses of the PolD–PCNA–DNA complex revealed that residues 1000–1205 of the DP2 C-terminal domain are well-ordered and contain a conserved α1–Zn–α2–α3 structure (25,43) that complexes with DP1 (interactions between the regions shown in magenta and cyan in Figure 5B, Supplementary Figure S2). In contrast, residues 1206 to 1324 are disordered and seem to move flexibly. A variant C-terminal domain lacking the tail (1000–1205) abrogated PriL–DP2 interaction (Figure 5A), suggesting that the interaction site is located between residues 1206–1324 of DP2.

The interface of the C-terminal domain of DP2 and DP1 in the archaeal PolD is conserved in the eukaryotic family-B DNA polymerases. The C-terminal domain of the p180 subunit of Polα, for example, interacts with p70 (Figure 5B) (28). It also binds PriL via a conserved hydrophobic motif at the extreme C-terminus of p180 (Figure 5B, C) (12). We found a similar hydrophobic motif at the C-terminus of DP2 (Figure 5C, Supplementary Figure S2). A recent study on *P. abyssi* proteins also mentioned this homology and reported primase interaction with the C-terminal peptide of DP2 (42). They also named the hydrophobic motif cPIP (canonical PIP) because it interacts with PCNA (40–42). To determine whether these hydrophobic amino acids contribute to complex formation, we performed gel-filtration chromatography analysis and confirmed that PolD and primase eluted with different retention time depending on their molecular sizes (Figure 5D). Under the same conditions, a mixture of PolD and primase yielded a single peak corresponding to the predicted molecular weight of the PolD–primase complex. However, truncation of the 11 C-terminal amino acids from DP2 (1314-KGISLDEFFGS-1324) abolished complex formation. We introduced amino acid substitutions (L1318A/F1321A/F1322A) to validate the importance of the conserved sequence of cPIP. The mutant PolD was eluted separately from the primase in the gel filtration chromatography with the same condition. (Supplementary Figure S3A). Thus, *T. kodakarensis* PolD forms a stable complex with primase in solution mainly via interaction at cPIP in DP2.

PolD changes binding partners from primase to PCNA depending on DNA

The stable complex formation suggested that PolD and primase function together as a primosome in *T. kodakarensis.* However, PolD also works as replicase to processively synthesize nascent DNA strands after primer formation. Therefore, an important question is how PolD is involved in both primer synthesis and processive strand elongation. We identified the primase interaction motif at the C-terminus of DP2 (Figure 5) and found it is identical to the PIP-box motif of DP2 (40,41). To determine whether primase–PCNA binding is cooperative or competitive, we analysed an equimolar mixture of these proteins by gel-filtration chromatography. The PolD–primase complex eluted together, and PCNA eluted separately (Figure 6A). It is reasonable to conclude that PolD preferentially binds primase rather than PCNA because *T. kodakarensis* PolD associated with PCNA with a K_D of 4.8×10^{-7} M (43), approximately 10-fold higher than the K_D for PolD-primase (Figure 4B).

T. kodakarensis PCNA exists as a monomer in solution (41,56) but assembles on dsDNA as a trimeric ring. Our recent structural analysis showed that residue E171 in each subunit of the PCNA-trimer binds to PolD, in addition to the PIP-mediated interaction, resulting in the formation of the constitutive PolD–PCNA–DNA complex (43). We added a primed-DNA to a solution of primase, PCNA and PolD to investigate whether the binding affinities change in the presence of DNA. Gel-filtration chromatography showed that PolD preferentially bound PCNA

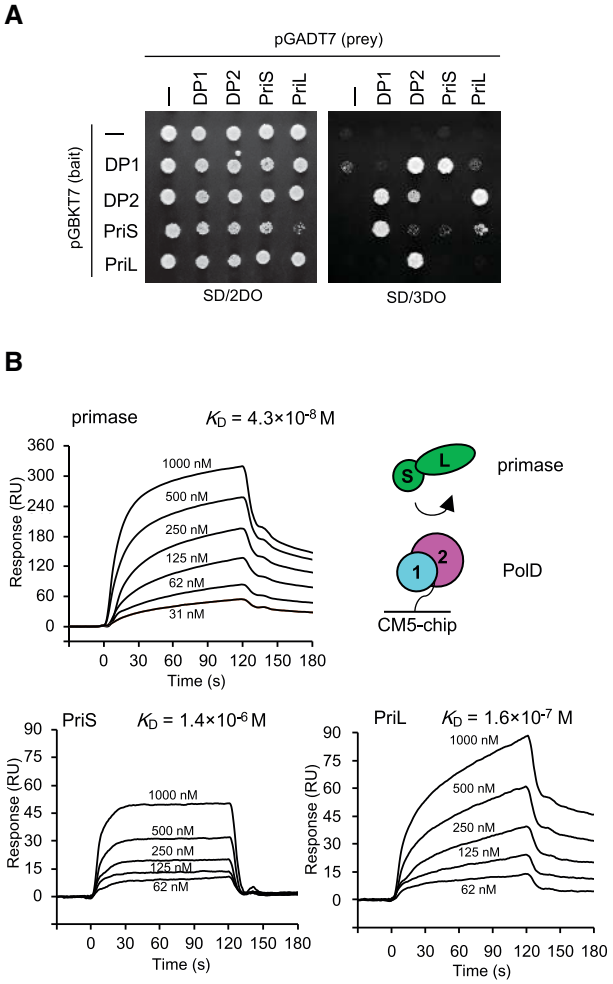

Figure 4. DP1 and DP2 subunits of DNA polymerase (PolD) interact with PriS and PriL subunits of primase, respectively. (**A**) The interaction between PolD (DP1, DP2) and primase (PriS, PriL) was analysed by a yeast two-hybrid assay. Cell suspensions were spotted onto SD plates without Leu and Trp (SD/2DO, left) and Leu, Trp and His (SD/3DO, right). Minus indicates the transformants with the bait or prey plasmid without insert DNA. (**B**) Surface plasmon resonance (SPR) analyses of primase (PriS–PriL), PriS or PriL with the PolD-bound chip. Indicated concentrations of primase, PriS or PriL were loaded onto the PolD-immobilized chip. The apparent equilibrium constants (K_D) are shown at the top of the sensorgram.

and DNA, and primase eluted separately (Figure 6B). The PolD–primase complex was isolated by gel filtration (Figure 6C), and PCNA and DNA were added to confirm the partner exchange of primase to PCNA. PolD eluted with PCNA and DNA, and primase eluted separately (Figure 6C). These results suggest that PolD preferentially complexes with primase to start primer synthesis, then the DNA-loaded PCNA ejects the primase from PolD to form a PolD–PCNA–DNA complex.

PCNA binding to another PIP-motif is the trigger to release primase for the functional elongation complex

A recent report showed that *P. abyssi* PolD contains a PCNA binding site, iPIP, in the C-terminal domain of DP2, in addition to cPIP (Supplementary Figure S2), which is important for primase and PCNA binding, and that PCNA switches to bind iPIP for processive elongation (42). Comparison of the recently reported PolD structures from *T. kodakarensis* (PDB 6KNB) and *P. abyssi* (PDB 6T8H) showed the similarity of the overall structures, including the C-terminal regions (Supplementary Figure S4). We investigated the interactions of *T. kodakarensis* DP2 with primase and PCNA in greater detail. We constructed an iPIP mutant (Q1206A/L1209A/M1210A) and a cPIP mutant (L1318A/F1321A/F1322A), and used them for the gel filtration experiment (Supplementary Figure S3). The mutation at iPIP did not affect PolD–primase complex formation, but the mutation at cPIP disrupted the interaction. A slightly retained binding may be due to the interaction between DP1 and PriS as shown in this study. In contrast, the PolD–PCNA–DNA complex was formed despite mutations in cPIP, but iPIP mutations disrupted the complex (Supplementary Figure S3B), suggesting that iPIP is essential for stable complex formation with PCNA. A weaker band of PCNA was detected in the same fraction of PolD iPIP mutant (Supplementary Figure S3B). It should be due to the interaction at E171 of PCNA, or intact cPIP, as described above. Using this iPIP mutant, we investigated the exchange mechanism from primase to PCNA. We found that the DNA-dependent partner exchange from primase to PCNA, observed for the wild type PolD, was not detected when the iPIP mutant PolD was used (Figure 6D). These results suggest that primase preferentially binds cPIP and blocks PCNA binding. However, the C-terminal region of DP2 is flexible and may change its conformation to allow PCNA to bind iPIP after primer synthesis.

DISCUSSION

Interactions between GINS and GAN (31–33), MCM and GINS (31–34), PolD and primase (36,42), and PolD and GINS (35–37) have been reported as mediators of DNA replication in several Archaea. The MCM–GINS–GAN complex has also been reported as a replicative CMG-like helicase (32–34). These analyses let us consider a structural model of the archaeal replisome, and we investigated the molecular interactions of the proteins related to DNA replication. This report is the first direct demonstration of the archaeal primase-polymerase-helicase complex using purified proteins.

Our *in vitro* analyses demonstrated that *T. kodakarensis* PolD and primase made a four-subunit complex comprised of DP1, DP2, PriS and PriL. Furthermore, primase-bound PolD simultaneously bound GINS, a component of CMG helicase. This primase–polymerase–helicase connection should form a functional replisome for the efficient progress of the sequential reaction of double-strand dissociation, primer synthesis and strand extension. Unlike *S. solfataricus*, in which primase binds to the Gins23 subunit of GINS (54), *T. kodakarensis* primase does not directly bind GINS. Among the Archaea, only the Crenarchaea do not possess PolD and instead utilize three-family B DNA polymerases (58). A different mechanism of replisome assembly may be functional in Crenarchaeota.

We showed that all four subunits contributed to PolD–primase complex assembly via interactions of DP1–PriS

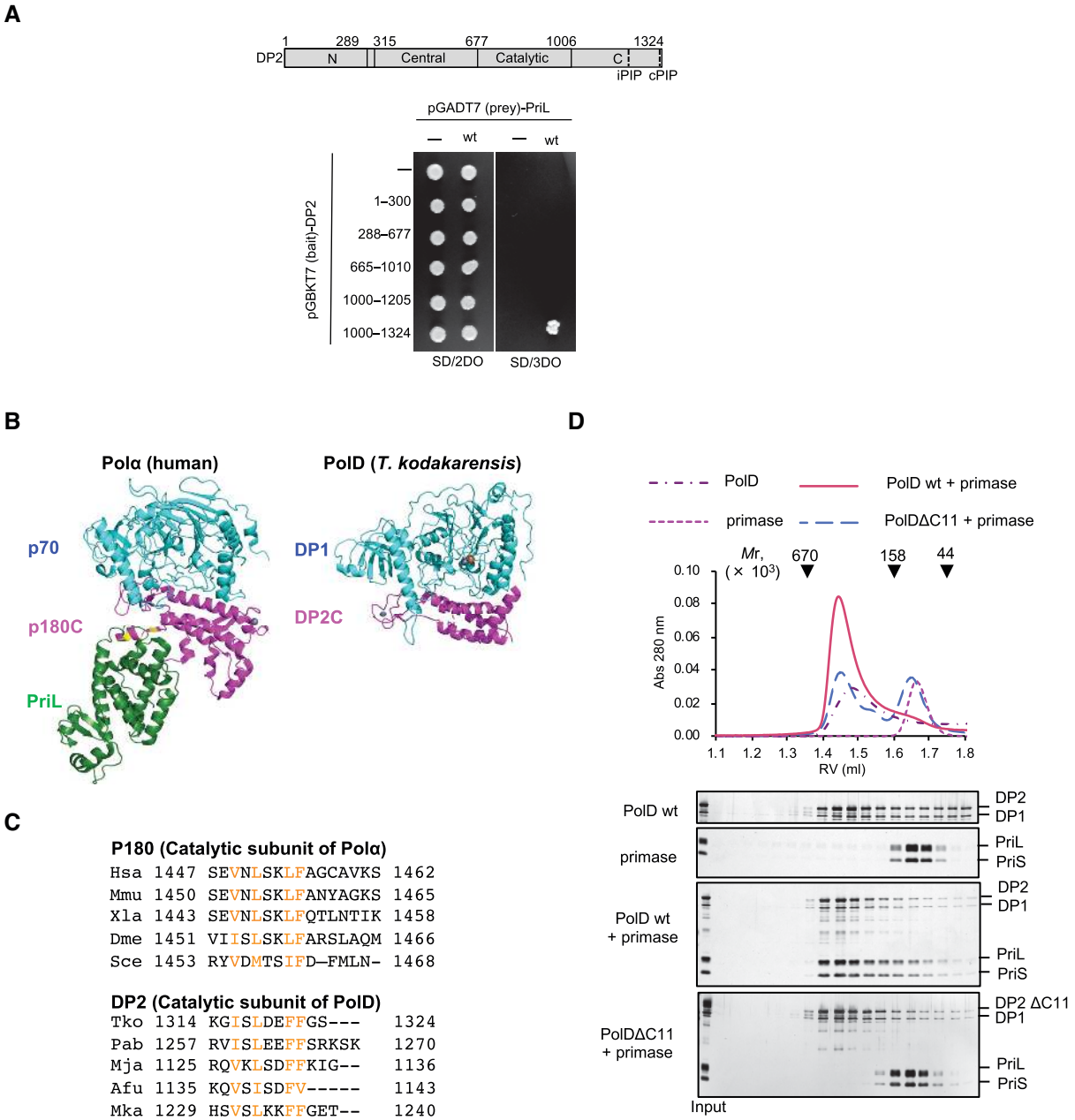

Figure 5. A conserved hydrophobic motif at the C-terminus of DP2 is critical for the interaction with primase. (**A**) The interactions between various DP2 fragments and PriL were analysed by a yeast two-hybrid assay. Domain organisation of DP2 was schematically shown. (**B**) Structural comparison of the DNA polymerase (PolD) (DP1–DP2C) from *T. kodakarensis* (PDB 6KNB) and Polα-primase (p70–p180–PriL) from Homo sapience (PDB 5EXR). B-subunits (DP1 and p70), catalytic subunits (DP2 and p180) and PriL are cyan, magenta and green, respectively. The conserved hydrophobic amino acids in the C-terminus of p180 are orange. (**C**) Multiple sequence alignments of the C-terminus of p180 and DP2. (Hsa: *Homo sapiens*; Mmu: *Mus musculus*; Xla: *Xenopus laevis*; Dme: *Drosophila melanogaster*; Sce: *Saccharomyces cerevisiae*; Tko: *Thermococcus kodakarensis*; Pab: *Pyrococcus abyssi*; Mja: *Methanocaldococcus jannaschii*; Afu: *Archaeoglobus fulgidus*; Mac: *Methanosarcina acetivorans*; Mka: *Methanopyrus kandleri*). The conserved hydrophobic motif is orange. Amino acid sequences of p180 and DP2 from indicated species were aligned using MAFFT-E-INS-I, and the C-terminal regions are shown. (**D**) The interaction of PolD (wt or ΔC11) with primase was analysed by gel-filtration chromatography.

and DP2–PriL. Critically, a hydrophobic motif (PIP-box) at the extreme C-terminus of DP2 was essential for the interaction with PriL. The hydrophobic amino acids in DP2 are widely conserved in Archaea, and even in the eukaryotic Polα (Figure 5, Supplementary Figure S2). The crystal structure of the human primosome revealed that the p180 subunit of Polα interacts with PriL via the C-terminal peptide (51). Also, truncation of the C-terminal 16 amino acids in yeast Pol1 abolished the interaction with primase (12), and the MBP-fused C-terminal region interacts with primase with a K_D of 245 nM, which is similar to the affinity of PolD–PriL (K_D 160 nM) in this study. In human p180, C-terminal truncation did not completely abrogate the interaction with primase (59), indicating the possibility of the

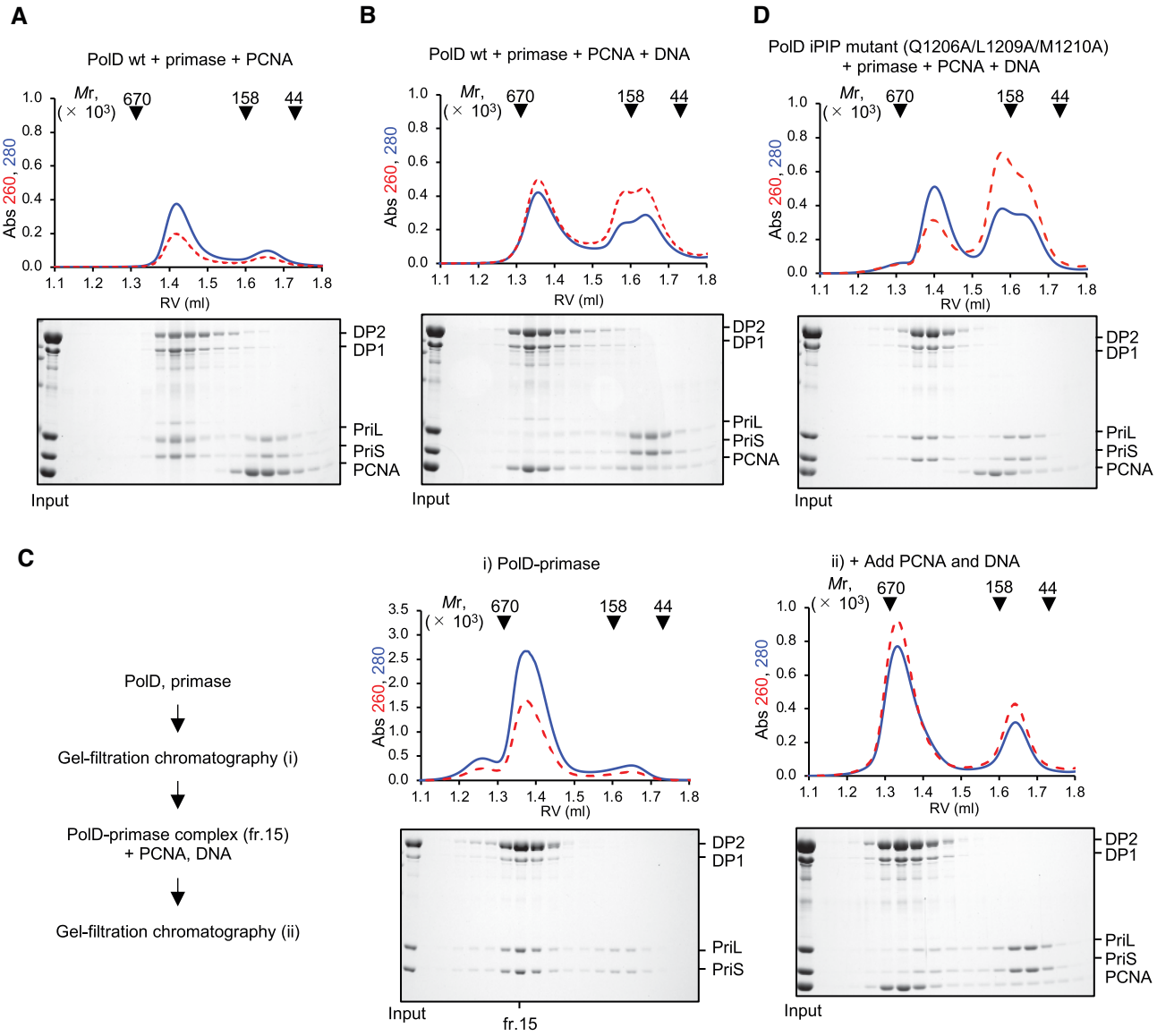

Figure 6. DNA polymerase (PolD) dissociates from primase to make a PolD–proliferating cell nuclear antigen (PCNA)–DNA ternary complex. (**A**–**B**) Complex formation of PolD, primase and PCNA in the presence (**A**) or absence (**B**) of DNA were analysed. (**C**) Complex formation of PolD, primase, PCNA and DNA was analysed by gel-filtration chromatographies. The PolD–primase complex was isolated (i), and then the fraction containing pure PolD–primase complex (fr. 15) was mixed with PCNA and DNA to be subjected to gel-filtration chromatography again (ii). (**D**) The iPIP mutant (Q1206A/L1209A/M1210A) was used instead of wild type PolD. The elution profiles, monitored by the absorbance at 260 and 280 nm, are shown in the dashed red and solid blue lines, respectively. Each fraction was separated by 10% SDS-PAGE, followed by staining.

second interaction site between them as we reported here between *T. kodakarensis* DP1 and PriS.

Our cryo-EM analysis of PolD–primase supported the results of these biochemical analyses. Combined with our current knowledge related to the primase complex including this study, we built a 3D model of the initiation complex containing PolD, primase and primer-template (Supplementary Figure S5, Figure 7A). Since the protrusion from the OB domain of DP1 exhibited a flat shape (Figure 1D, E), we assigned this protrusion as a part of PriS subunit though the size is a little smaller than the expected size of PriS. We assumed the density of the rest of PriS and the entire PriL regions are smeared out during the averaging process of single-particle analysis, because the PriL side is bound to DP2 via its flexible loop, thus enabling dynamic movement of this area. We have tried several methods including masked 3D classification (60) and multi-body refinement (61), which are used for improving maps containing a flexible heterogeneous region (or heterogeneous structures). However, none of these methods improved PriS–PriL density most likely due to the dynamic movement of the primase area. It is possible that PriL is not present in all particles, but the PriS–PriL complex is stable from our biochemical analysis, and these two proteins are not likely separated in the protein samples. The C-terminal region (CTD) of PriL holds the 5′ terminus of the synthesizing primer (51,62). Therefore, it is expected that the PriL–CTD position will move as the primer extends because the active site

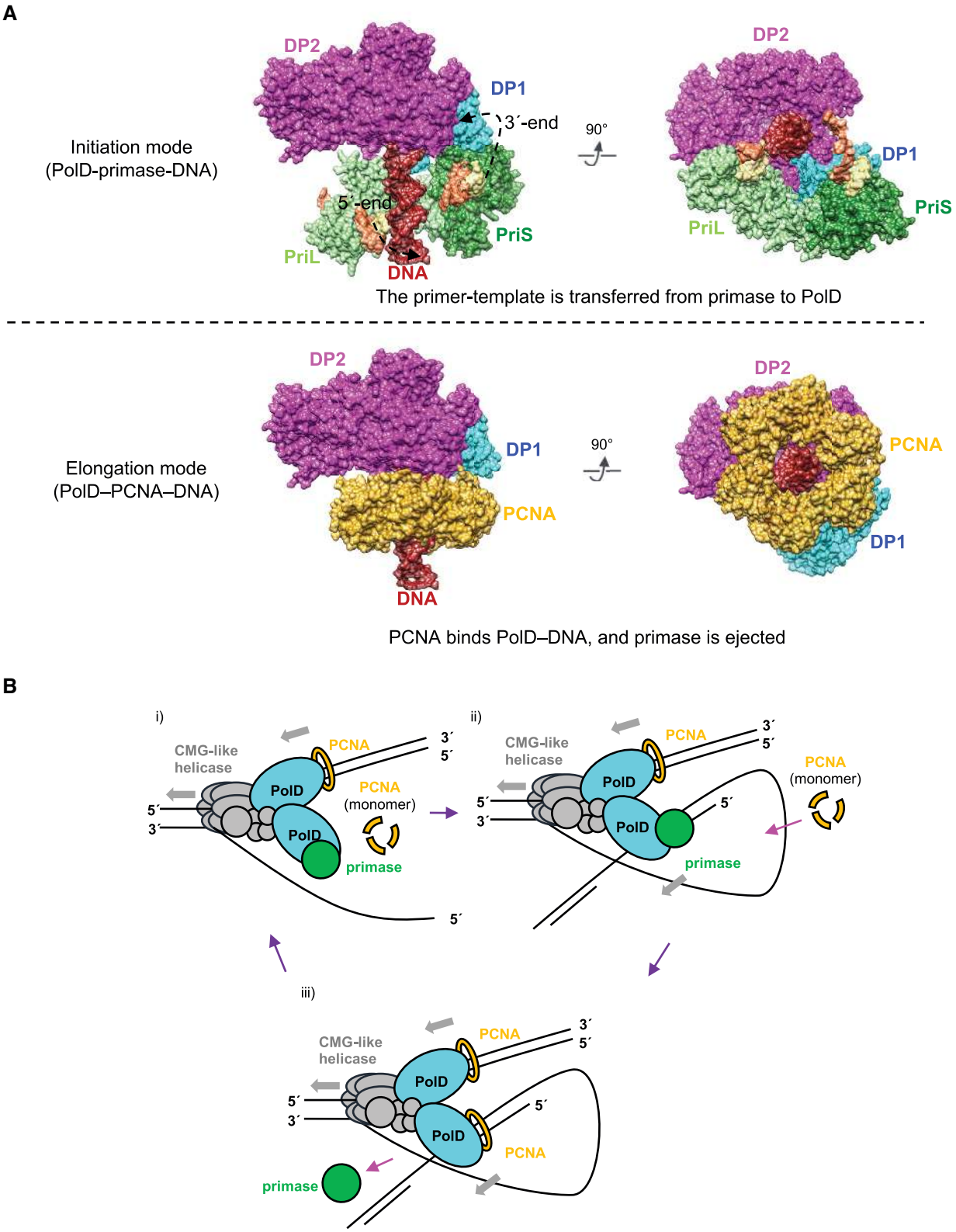

Figure 7. Interactions of DNA polymerase (PolD) with primase and proliferating cell nuclear antigen (PCNA) to switch functional mode from initiation to elongation in the archaeal replisome. (**A**) The atomic models for the primase ejection. Assumed docking model of PolD–primase–DNA complex (upper) and published structure of PolD–PCNA–DNA complex (pdb: 6knb) (lower) are shown. DP1, DP2, PriS, PriL and PCNA are depicted with surface models, cyan, magenta, green, light green and yellow. PolD-bound DNA strand is in brown, and the Primer–template, which binds primase, is in khaki (RNA primer) and orange (DNA template). (**B**) Model of the archaeal replisome. While PolD for leading-strand makes a complex with PCNA to synthesize nascent strand processively, PolD for lagging-strand changes the interaction partner dynamically. i) In the absence of DNA, PolD make a stable complex with primase to form a primosome. ii) PolD-primase initiates primer synthesis. iii) PCNA-trimer binds dsDNA and PolD to start processive extension. Primase is ejected from the complex.

in PriS stays in place by interaction with DP1. Further efforts are required to observe the complex structure more precisely.

Although human Polα forms a constitutive complex with primase as the initiation-specific enzyme, PolD must interact with PCNA and primase for the dual functions of initiation and elongation. Intriguingly, the primase-interacting site of DP2 has been reported as the PIP-box responsible for the interaction with PCNA (40,63). Our results supported the recent report of *P. abyssi* PolD (42) and demonstrated the partner exchange on PolD from primase to PCNA in *T. kodakarensis* replisome. PolD preferentially bound primase rather than PCNA to work as an initiation complex, and subsequently releases primase to make a PolD–PCNA–DNA complex for the processive elongation (Figure 6).

With the atomic model of the PolD-primase initiation complex described here and the PolD–PCNA–DNA elongation complex structure (43), we propose a detailed switching model (Figure 7). Before capturing the template strand, PolD connects primase to the CMG helicase for lagging-strand synthesis, while leading-strand PolD processively extends a nascent strand with PCNA (Figure 7B-i). As primase preferentially binds single-stranded DNA (3), primosome binds a template strand unwound by CMG helicase (62) to initiate *de novo* primer synthesis (Figure 7B-ii). During RNA primer synthesis, PriL binds to the 5′-triphosphate of an RNA primer, and PriS incorporates ribonucleotides at the 3′-OH end (primase-bound template-primer is orange in Figure 7A) (51,62,64). PriL restricts the length of the RNA primer to the length between PriL-CTD and PriS (61). Therefore, when the synthesized primer reaches the upper limit, the active site of PriS releases the 3′-OH end of the primer so that PolD can grasp it and start extension (PolD-bound template-primer is brown in Figure 7A). In our model, substrate transfer can be conducted by simply sliding the 3′ end into the active site of DP2 along the surface made by PriS and DP1. The DNA strand extension makes dsDNA long enough to load PCNA. The PCNA protomer then assembles to form a ring structure on the DNA and binds PolD to start processive extension (Figure 7A, B-iii). For this event, primase should be ejected from the complex by PCNA, and iPIP is needed for PCNA to remove primase from PolD (Figure 6). Our model suggests that primase and PCNA bind the same region of PolD, and therefore, PCNA binding to iPIP could sterically hinder the binding of primase (Figure 7A). It is unknown whether PCNA ejects cPIP-bound primase first or if iPIP-binding is needed for PCNA to eject primase from the cPIP site.

In Eukarya, RFC (Replication Factor C) mediates polymerase switching from Polα to Polδ by displacing Polα and loading PCNA to recruit Polδ (65,66). In our model, PolD functions as Polα to Polδ, and polymerase switching is not needed. Instead, PolD changes its partners from primase to PCNA. RFC is not necessarily required for loading PCNA from the hyperthermophilic Archaea onto DNA to stimulate DNA polymerase *in vitro* (40,41), because of fewer hydrogen bonds at the intermolecular interfaces of PCNA-trimer, compared with that in Eukarya (67,68). Therefore, RFC may not be involved in loading PCNA onto the dsDNA synthesized by PolD-primase in our proposed mechanism. When PolD–PCNA encounters a downstream Okazaki fragment, PCNA can recruit FEN1 (Flap Endonuclease 1), and DNA Ligase (69). The interaction of PolD and GINS is stable, and therefore, PolD may dissociate from PCNA and recycle to form a complex with primase again for the next Okazaki fragment (Figure 7B-i).

We presented a model and possible mechanism, in which PolD exchanges partners to switch its function from initiation to elongation mode from our *in vitro* studies here. Further studies are required to investigate whether this exchange mechanism functions *in vivo*. Mutation studies in the genes on the *T. kodakarensis* genome will provide useful information to evaluate the fidelity of our model.

DATA AVAILABILITY

The structure of the PolD–primase complex obtained by this study are deposited into the EMData Bank (accession code: EMD-30937).

SUPPLEMENTARY DATA

Supplementary Data are available at NAR Online.

ACKNOWLEDGEMENTS

We thank Yalu Tang for technical assistance. We also thank the members of the cryo-EM facility in KEK for cryo-EM data collection. This work was partly performed in the Cooperative Research Project Program of the Medical Institute of Bioregulation, Kyushu University. The authors would like to thank Enago (WWW.enago.jp) for the English language review.

FUNDING

Grant-in-Aid for Japan Society for the Promotion of Science (JSPS) Fellows [JP20J12260 to K.O.], and also by JSPS KAKENHI [JP26242075 to Y.I., JP18K05442 to S.I., JP18K06089, JP16H01410 to K.Ma., JP17H01818 to T.S.]; JST PRESTO [JPMJPR12L9 to K.M.]; Platform Project for Supporting Drug Discovery and Life Science Research (Basis of Supporting Innovative Drug Discovery and Life Science Research) from AMED [JP19am0101069 support number 0673 to T.S., JP21am0101071 support number 2054 to Senda, KEK]. Funding for open access charge: research grant JP20J12260.
Conflict of interest statement. None declared.

REFERENCES

1. Bergsch,J., Allain,F.H. and Lipps,G. (2019) Recent advances in understanding bacterial and archaeoeukaryotic primases. *Curr. Opin. Struct. Biol.*, **59**, 159–167.
2. Bocquier,A., Liu,L., Cann,I., Kohda,D. and Ishino,Y. (2001) Archaeal primase: bridging the gap between RNA and DNA polymerase. *Curr. Biol.*, **11**, 452–456.
3. Liu,L., Komori,K., Ishino,S., Bocquier,A., Cann,I., Kohda,D. and Ishino,Y. (2001) The archaeal DNA primase: biochemical characterization of the p41-p46 complex from *Pyrococcus furiosus*. *J. Biol. Chem.*, **276**, 45484–45490.
4. Matsunaga,F., Norais,C., Forterre,P. and Myllykallio,H. (2003) Identification of short 'eukaryotic' Okazaki fragments synthesized from a prokaryotic replication origin. *EMBO Rep.*, **4**, 154–158.

5. Kelman,L.M. and Kelman,Z. (2014) Archaeal DNA replication. *Annu. Rev. Genet.*, **48**, 71–97.
6. Greci,M.D. and Bell,S.D. (2020) Archaeal DNA replication. *Annu. Rev. Microbiol.*, **74**, 65–80.
7. Lujan,S.A., Williams,J.S. and Kunkel,T.A. (2016) DNA polymerases divide the labor of genome replication. *Trends Cell Biol.*, **26**, 640–654.
8. Brooke,R.G. and Dumas,L.B. (1991) Reconstitution of the *Saccharomyces cerevisiae* DNA primase-DNA polymerase protein complex *in vitro*. The 86-kDa subunit facilitates but is not required for complex formation. *J. Biol. Chem.*, **266**, 10093–10098.
9. Simon,A.C., Zhou,J.C., Perera,R.L., van Deursen,F., Evrin,C., Ivanova,M.E., Kilkenny,M.L., Renault,L., Kjaer,S., Matak-Vinkovic,D. *et al.* (2014) A Ctf4 trimer couples the CMG helicase to DNA polymerase alpha in the eukaryotic replisome. *Nature*, **510**, 293–297.
10. Pellegrini,L. (2012) The Polα-primase complex. *Subcell. Biochem.*, **62**, 157–169.
11. Nunez-Ramirez,R., Klinge,S., Sauguet,L., Melero,R., Recuero-Checa,M.A., Kilkenny,M., Perera,R.L., Garcia-Alvarez,B., Hall,R.J., Nogales,E. *et al.* (2011) Flexible tethering of primase and DNA Polα in the eukaryotic primosome. *Nucleic Acids Res.*, **39**, 8187–8199.
12. Kilkenny,M.L., De Piccoli,G., Perera,R.L., Labib,K. and Pellegrini,L. (2012) A conserved motif in the C-terminal tail of DNA polymerase α tethers primase to the eukaryotic replisome. *J. Biol. Chem.*, **287**, 23740–23747.
13. Pursell,Z.F., Isoz,I., Lundström,E.B., Johansson,E. and Kunkel,T.A. (2007) Yeast DNA polymerase ε participates in leading-strand DNA replication. *Science*, **317**, 127–130.
14. Nick McElhinny,S.A., Gordenin,D.A., Stith,C.M., Burgers,P.M. and Kunkel,T.A. (2008) Division of labor at the eukaryotic replication fork. *Mol. Cell*, **30**, 137–144.
15. Kelman,Z. and Hurwitz,J. (1998) Protein-PCNA interactions: a DNA-scanning mechanism? *Trends Biochem. Sci.*, **23**, 236–238.
16. Handa,T., Kanke,M., Takahashi,T.S., Nakagawa,T. and Masukata,H. (2012) DNA polymerization-independent functions of DNA polymerase ε in assembly and progression of the replisome in fission yeast. *Mol. Biol. Cell*, **23**, 3240–3253.
17. Sengupta,S., van Deursen,F., de Piccoli,G. and Labib,K. (2013) Dpb2 integrates the leading-strand DNA polymerase into the eukaryotic replisome. *Curr. Biol.*, **23**, 543–552.
18. Huang,M.E., Le Douarin,B., Henry,C. and Galibert,F. (1999) The *Saccharomyces cerevisiae* protein YJR043C (Pol32) interacts with the catalytic subunit of DNA polymerase α and is required for cell cycle progression in G2/M. *Mol. Gen. Genet.*, **260**, 541–550.
19. Garbacz,M.A., Lujan,S.A., Burkholder,A.B., Cox,P.B., Wu,Q., Zhou,Z.X., Haber,J.E. and Kunkel,T.A. (2018) Evidence that DNA polymerase δ contributes to initiating leading strand DNA replication in *Saccharomyces cerevisiae*. *Nat. Commun.*, **9**, 858.
20. Zhou,Z.X., Lujan,S.A., Burkholder,A.B., Garbacz,M.A. and Kunkel,T.A. (2019) Roles for DNA polymerase δ in initiating and terminating leading strand DNA replication. *Nat. Commun.*, **10**, 3992.
21. Suwa,Y., Gu,J., Baranovskiy,A.G., Babayeva,N.D., Pavlov,Y.I. and Tahirov,T.H. (2015) Crystal structure of the human Polα B Subunit in complex with the C-terminal domain of the catalytic subunit. *J. Biol. Chem.*, **290**, 14328–14337.
22. Baranovskiy,A.G., Gu,J., Babayeva,N.D., Kurinov,I., Pavlov,Y.I. and Tahirov,T.H. (2017) Crystal structure of the human Polε B-subunit in complex with the C-terminal domain of the catalytic subunit. *J. Biol. Chem.*, **292**, 15717–15730.
23. Baranovskiy,A.G., Babayeva,N.D., Liston,V.G., Rogozin,I.B., Koonin,E.V., Pavlov,Y.I., Vassylyev,D.G. and Tahirov,T.H. (2008) X-ray structure of the complex of regulatory subunits of human DNA polymerase δ. *Cell Cycle*, **7**, 3026–3036.
24. Tahirov,T.H., Makarova,K.S., Rogozin,I.B., Pavlov,Y.I. and Koonin,E.V. (2009) Evolution of DNA polymerases: an inactivated polymerase-exonuclease module in Polε and a chimeric origin of eukaryotic polymerases from two classes of archaeal ancestors. *Biol. Direct*, **4**, 11.
25. Raia,P., Carroni,M., Henry,E., Pehau-Arnaudet,G., Brule,S., Beguin,P., Henneke,G., Lindahl,E., Delarue,M. and Sauguet,L. (2019) Structure of the DP1-DP2 PolD complex bound with DNA and its implications for the evolutionary history of DNA and RNA polymerases. *PLoS Biol.*, **17**, e3000122.
26. Uemori,T., Sato,Y., Kato,I., Doi,H. and Ishino,Y. (1997) A novel DNA polymerase in the hyperthermophilic archaeon, *Pyrococcus furiosus*: gene cloning, expression, and characterization. *Genes Cells*, **2**, 499–512.
27. Makarova,K.S., Krupovic,M. and Koonin,E.V. (2014) Evolution of replicative DNA polymerases in archaea and their contributions to the eukaryotic replication machinery. *Front Microbiol.*, **5**, 354.
28. Cubonova,L., Richardson,T., Burkhart,B.W., Kelman,Z., Connolly,B.A., Reeve,J.N. and Santangelo,T.J. (2013) Archaeal DNA polymerase D but not DNA polymerase B is required for genome replication in *Thermococcus kodakarensis*. *J. Bacteriol.*, **195**, 2322–2328.
29. Sarmiento,F., Mrazek,J. and Whitman,W.B. (2013) Genome-scale analysis of gene function in the hydrogenotrophic methanogenic archaeon *Methanococcus maripaludis*. *Proc. Natl. Acad. Sci. U.S.A.*, **110**, 4726–4731.
30. Li,Z., Pan,M., Santangelo,T.J., Chemnitz,W., Yuan,W., Edwards,J.L., Hurwitz,J., Reeve,J.N. and Kelman,Z. (2011) A novel DNA nuclease is stimulated by association with the GINS complex. *Nucleic. Acids. Res.*, **39**, 6114–6123.
31. Makarova,K.S., Koonin,E.V. and Kelman,Z. (2012) The CMG (CDC45/RecJ, MCM, GINS) complex is a conserved component of the DNA replication system in all archaea and eukaryotes. *Biol. Direct*, **7**, 7.
32. Xu,Y., Gristwood,T., Hodgson,B., Trinidad,J.C., Albers,S.-V. and Bell,S.D. (2016) Archaeal orthologs of Cdc45 and GINS form a stable complex that stimulates the helicase activity of MCM. *Proc. Natl. Acad. Sci. U.S.A.*, **113**, 13390–13395.
33. Nagata,M., Ishino,S., Yamagami,T., Ogino,H., Simons,J-R., Kanai,T., Atomi,H. and Ishino,Y. (2017) The Cdc45/RecJ-like protein forms a complex with GINS and MCM, and is important for DNA replication in *Thermococcus kodakarensis*. *Nucleic. Acids. Res.*, **45**, 10693–10705.
34. Ogino,H., Ishino,S., Kohda,D. and Ishino,Y. (2017) The RecJ2 Protein in the thermophilic archaeon, *Thermoplasma acidophilum* is a 3′–5′ exonuclease and associates with a DNA replication complex. *J. Biol. Chem.*, **292**, 7921–7931.
35. Li,Z., Santangelo,T.J., Cubonova,L., Reeve,J.N. and Kelman,Z. (2010) Affinity purification of an archaeal DNA replication protein network. *mBio*, **1**, e00221-10.
36. Pluchon,P.F., Fouqueau,T., Creze,C., Laurent,S., Briffotaux,J., Hogrel,G., Palud,A., Henneke,G., Godfroy,A., Hausner,W. *et al.* (2013) An extended network of genomic maintenance in the archaeon *Pyrococcus abyssi* highlights unexpected associations between eucaryotic homologs. *PLoS One*, **8**, e79707.
37. Lu,S., Zhang,X., Chen,K., Chen,Z., Li,Y., Qi,Z., Shen,Y. and Li,Z. (2019) The small subunit of DNA polymerase D (DP1) associates with GINS-GAN complex of the thermophilic archaea in *Thermococcus* sp. 4557. *Microbiologyopen*, **8**, e00848.
38. Henneke,G., Flament,D., Hubscher,U., Querellou,J. and Raffin,J.P. (2005) The hyperthermophilic euryarchaeota *Pyrococcus abyssi* likely requires the two DNA polymerases D and B for DNA replication. *J. Mol. Biol.*, **350**, 53–64.
39. Ishino,S. and Ishino,Y. (2006) Comprehensive search for DNA polymerase in the hyperthermophilic archaeon, *Pyrococcus furiosus*. *Nucleosides Nucleotides Nucleic Acids*, **25**, 681–691.
40. Tori,K., Kimizu,M., Ishino,S. and Ishino,Y. (2007) DNA polymerases BI and D from the hyperthermophilic archaeon *Pyrococcus furiosus* both bind to proliferating cell nuclear antigen with their C-terminal PIP-box motifs. *J. Bacteriol.*, **189**, 5652–5657.
41. Kuba,Y., Ishino,S., Yamagami,T., Tokuhara,M., Kanai,T., Fujikane,R., Daiyasu,H., Atomi,H. and Ishino,Y. (2012) Comparative analyses of the two proliferating cell nuclear antigens from the hyperthermophilic archaeon, *Thermococcus kodakarensis*. *Genes Cells*, **17**, 923–937.
42. Madru,C., Henneke,G., Raia,P., Hugonneau-Beaufet,I., Pehau-Arnaudet,G., England,P., Lindahl,E., Delarue,M., Carroni,M. and Sauguet,L. (2020) Structural basis for the increased processivity of D-family DNA polymerases in complex with PCNA. *Nat. Commun.*, **11**, 1591.
43. Mayanagi,K., Oki,K., Miyazaki,N., Ishino,S., Yamagami,T., Morikawa,K., Iwasaki,K., Kohda,D., Shirai,T. and Ishino,Y. (2020)

Two conformations of DNA polymerase D–PCNA–DNA, an archaeal replisome complex, revealed by cryo-electron microscopy. *BMC Biol.*, **18**, 152.
44. Zheng,S.Q., Palovcak,E., Armache,J.P., Verba,K.A., Cheng,Y. and Agard,D.A. (2017) MotionCor2: anisotropic correction of beam-induced motion for improved cryo-electron microscopy. *Nat. Methods*, **14**, 331–332.
45. Zhang,K. (2016) Gctf: Real-time CTF determination and correction. *J. Struct. Biol.*, **193**, 1–12.
46. Wagner,T., Merino,F., Stabrin,M., Moriya,T., Antoni,C., Apelbaum,A., Hagel,P., Sitsel,O., Raisch,T., Prumbaum,D. *et al.* (2019) SPHIRE-crYOLO is a fast and accurate fully automated particle picker for cryo-EM. *Commun. Biol.*, **2**, 218.
47. Scheres,S.H.W. (2012) RELION: Implementation of a Bayesian approach to cryo-EM structure determination. *J. Struct. Biol.*, **180**, 519–530.
48. Webb,B. and Sali,A. (2016) Comparative protein structure modeling using MODELLER. *Curr. Protoc. Bioinformatics*, **54**, 5.6.1–5.6.37.
49. Lao-Sirieix,S., Nookala,R.K., Roversi,P., Bell,S.D. and Pellegrini,L. (2005) Structure of the heterodimeric core primase. *Nat. Struct. Mol. Biol.*, **12**, 1137–1144.
50. Ito,N., Nureki,O., Shirouzu,M., Yokoyama,S. and Hanaoka,F. (2003) Crystal structure of the *Pyrococcus horikoshii* DNA primase-UTP complex: implications for the mechanism of primer synthesis. *Genes Cells*, **8**, 913–923.
51. Baranovskiy,A.G., Babayeva,N.D., Zhang,Y., Gu,J., Suwa,Y., Pavlov,Y.I. and Tahirov,T.H. (2016) Mechanism of concerted RNA-DNA primer synthesis by the human primosome. *J. Biol. Chem.*, **291**, 10006–10020.
52. Mitkova,A.V., Khopde,S.M. and Biswas,S.B. (2003) Mechanism and stoichiometry of interaction of DnaG primase with DnaB helicase of *Escherichia coli* in RNA primer synthesis. *J. Biol. Chem.*, **278**, 52253–52261.
53. Lu,Y.B., Ratnakar,P.V., Mohanty,B.K. and Bastia,D. (1996) Direct physical interaction between DnaG primase and DnaB helicase of *Escherichia coli* is necessary for optimal synthesis of primer RNA. *Proc. Natl. Acad. Sci. U.S.A.*, **93**, 12902–12907.
54. Marinsek,N., Barry,E.R., Makarova,K.S., Dionne,I., Koonin,E.V. and Bell,S.D. (2006) GINS, a central nexus in the archaeal DNA replication fork. *EMBO Rep.*, **7**, 539–545.
55. Takashima,N., Ishino,S., Oki,K., Takafuji,M., Yamagami,T., Matsuo,R., Mayanagi,K. and Ishino,Y. (2019) Elucidating functions of DP1 and DP2 subunits from the *Thermococcus kodakarensis* family D DNA polymerase. *Extremophiles*, **23**, 161–172
56. Ladner,J.E., Pan,M., Hurwitz,J. and Kelman,Z. (2011) Crystal structures of two active proliferating cell nuclear antigens (PCNAs) encoded by *Thermococcus kodakaraensis*. *Proc. Natl. Acad. Sci. U.S.A.*, **108**, 2711–2716.
57. Oyama,T., Ishino,S., Fujino,S., Ogino,H., Shirai,T., Mayanagi,K., Saito,M., Nagasawa,N., Ishino,Y. and Morikawa,K. (2011) Architectures of archaeal GINS complexes, essential DNA replication initiation factors. *BMC Biol.*, **9**, 28.
58. Cooper,C.D.O. (2018) Archaeal DNA polymerases: new frontiers in DNA replication and repair. *Emerg. Top. Life Sci.*, **2**, 503–516.
59. Smith,R.W. and Nasheuer,H.P. (2002) Control of complex formation of DNA polymerase α-primase and cell-free DNA replication by the C-terminal amino acids of the largest subunit p180. *FEBS Lett.*, **527**, 143–146.
60. Scheres,S.H.W. (2016) Processing of structurally heterogeneous cryo-EM data in RELION. *Method Enzymol.*, **579**, 125–157.
61. Nakane,T., Kimanius,D., Lindahl,E. and Scheres,S.H.W. (2018) Characterisation of molecular motions in cryo-EM single-particle data by multi-body refinement in RELION. *elife*, **7**, e36861 .
62. Yan,J., Holzer,S., Pellegrini,L. and Bell,S.D. (2018) An archaeal primase functions as a nanoscale caliper to define primer length. *Proc. Natl. Acad. Sci. U.S.A.*, **115**, 6697–6702.
63. Castrec,B., Rouillon,C., Henneke,G., Flament,D., Querellou,J. and Raffin,J.P. (2009) Binding to PCNA in euryarchaeal DNA replication requires two PIP motifs for DNA polymerase D and one PIP motif for DNA polymerase B. *J. Mol. Biol.*, **394**, 209–218.
64. Baranovskiy,A.G., Zhang,Y., Suwa,Y., Gu,J., Babayeva,N.D., Pavlov,Y.I. and Tahirov,T.H. (2016) Insight into the human DNA primase interaction with template-primer. *J. Biol. Chem*, **291**, 4793–4802.
65. Mossi,R., Jónsson,Z.O., Allen,B.L., Hardin,S.H. and Hübscher,U. (1997) Replication factor C interacts with the C-terminal side of proliferating cell nuclear antigen. *J. Biol. Chem.*, **272**, 1769–1776.
66. Maga,G., Stucki,M., Spadari,S. and Hübscher,U. (2000) DNA polymerase switching: I. replication factor C displaces DNA polymerase α prior to PCNA loading. *J. Mol. Biol.*, **295**, 791–801.
67. Matsumiya,S., Ishino,Y. and Morikawa,K. (2001) Crystal structure of an archaeal DNA sliding clamp: proliferating cell nuclear antigen from *Pyrococcus furiosus*. *Prot. Sci.*, **10**, 17–23.
68. Matsumiya,S., Ishino,S., Ishino,Y. and Morikawa,K. (2003) Intermolecular ion pairs maintain toroidal structure of *Pyrococcus furiosus* PCNA. *Prot. Sci.*, **12**, 823–831.
69. Mayanagi,K., Ishino,S., Shirai,T., Oyama,T., Kiyonari,S., Kohda,D., Morikawa,K. and Ishino,Y. (2018) Direct visualization of DNA baton pass between replication factors bound to PCNA. *Sci. Rep.*, **8**, 16209.